



Review on optical, structural and electrical properties of ZnTe thin films: effect of deposition techniques, annealing and doping

Harinder Singh¹ · Tejbir Singh² · Jeewan Sharma¹

Received: 29 January 2018 / Revised: 17 May 2018 / Accepted: 21 June 2018 / Published online: 29 June 2018
© Institute of Smart Structures & Systems, Department of Aerospace Engineering, Indian Institute of Science, Bangalore, India 2018

Abstract

Zinc Telluride (ZnTe) has become a very fascinating research material for the scientists over past many years. This p type semiconducting material has a wide band gap, which makes it useful in many optoelectronic applications such as solar cells, light emitting diodes, laser screens etc. With the desire for eco-friendly alternative energy resources, it excites to investigate potential semiconducting materials at nano scale for solar cell applications. Due to direct, wide and controllable optical band gap of ZnTe with easy doping makes it a potential material for photoelectrochemical applications. In the present work, an attempt has been made to compile the work done by various researchers on optical properties (band gap, refractive index and absorption/transmission spectra, etc.), structural properties (crystallite/grain size, lattice constant and Zn:Te, etc.) and electrical properties (resistivity, activation energy, carrier concentration and hall mobility, etc.) of ZnTe thin films with main emphasis on the effect of deposition techniques, doping and annealing on these properties. Most of the thin films reported in literature shown polycrystalline cubic structure. It is found that annealed ZnTe thin films show enhanced optical, structural and electrical properties at different annealing temperatures. Doping methods used by various researchers have been discussed in detail and results show good doping impact on these properties as well.

Keywords Chalcogenide · Thin films · Polycrystalline · Doping · Annealing

Introduction

Elements from group II (metals) and group VI (chalcogens) of the periodic table forms the compound with semiconducting nature. Such semiconducting materials have attracted substantial attention in both fundamental research and technological applications (Mahmood et al. 2011; Singh et al. 2018a; Kshirsagar et al. 2013; Akkad and Abdulraheem 2013; Tanaka et al. 2018; Sharma et al. 2018; Sharma et al. 2017a). Amidst these compounds, Group IIB and group VI compounds such as ZnO, ZnS, ZnSe, ZnTe, CdO, CdS, CdSe, and CdTe are widely used in solar cells, semiconductor lasers, light emitting diodes, visible light photodetectors, nonlinear optical materials, magneto-

optical devices, radiation detectors and other optoelectronic applications (Contreras et al. 1999; Wu et al. 2001; Ramanathan et al. 2003; Schrier et al. 2007; Gangopadhyay et al. 2004; Shen et al. 2008; Jiao et al. 2006; Liu et al. 2006; Ruda 1992).

Chalcogenides form four elongated electron clouds around each atom. With hybridization of the *s*- and *p*-orbitals, the electron clouds have sp^3 configuration (Abrikosov et al. 1969). It makes the crystal lattice where atoms are tetrahedrally coordinated in such a way that every atom is symmetrically encircled by four nearest neighbor atoms of the other element. Hence, chalcogenides have cubic and hexagonal crystal structures (Ignatowicz and Kobendza 1981).

ZnTe is one of the most prominent materials among these wide-gap semiconductor compounds. It has potential to be used for preparing heterostructures with quantum-dimensional properties (Singh et al. 2018b). As it is transparent to photons of energy below 2.26 eV, which makes it nominee for a back contact of ZnTe based solar cells. ZnTe is used as an intermediate layer between

✉ Jeewan Sharma
jeewansharma29@gmail.com

¹ Thin Film Lab, Department of Nanotechnology, Sri Guru Granth Sahib World University, Fatehgarh Sahib, India

² Department of Physics, Sri Guru Granth Sahib World University, Fatehgarh Sahib, India

metallic back contact and CdTe absorber to improve the performance of CdTe thin films solar cells (Singh et al. 2018c). Due to the optimum direct band gap energy of 2.26 eV, ZnTe is chosen for light emitting diode (LED) applications (Tanaka et al. 2010; Millerd et al. 1996; Fang et al. 2009; Mochizuki et al. 1995; Sato and Katayama-Yoshida 2001; Smith et al. 1995). Furthermore, the band gap of ZnTe can be tuned in the visible region of electromagnetic spectrum (1.8–3.1 eV) which makes it a potential candidate in optoelectronic applications. Besides these properties, its additional advantages include potentially low cost, environmental stability and easily manufacturable (Kashyout et al. 1997; Nishio et al. 2001).

At the early stages, studies reflect that thin films possess significantly different properties as compare to same material in bulk form. Improvement in controlling the properties of the thin films in next years, revolutionized the use of thin films in electronic, opto-electronic and other devices. Scientists had explored compound semiconductor's thin films from more than 40 years. The potential of thin films of these semiconducting materials in high-performance electronic devices has been explored in terms of photovoltaic solar cells, non-linear optical detectors and laser screen materials (Bhargava 1997; Tamargo 2002; Sidorov et al. 2000; Mirov et al. 2007; Gessert et al. 1997). The size dependent properties were related with mechanical, optical, electrical, electronic and optoelectronic applications (Chandhuri and Pal 2001). The ZnTe nanostructured thin films with tunable optical band gap are of great interest for its use as window layer in the fabrication of solar cells (Ibrahim et al. 2004).

In the present article, an attempt has been made to compare the properties of ZnTe thin films synthesized by using different techniques. In particular, the effect of deposition techniques, annealing temperature and doping on the structural, optical and electrical properties of ZnTe thin films are reviewed, described in detail and tabulated. Furthermore, the importance of ZnTe thin films in various applications and its future scope are provided.

ZnTe deposition techniques

There are various methods used to synthesize ZnTe thin films. These methods are mainly classified in two categories viz. physical and chemical deposition techniques. Physical deposition technique includes thermal evaporation, e-beam evaporation, closed space sublimation and pulsed laser deposition technique, etc. Chemical deposition technique comprises electrodeposition, brush plating and spin coating techniques, etc. These techniques have been discussed briefly in the following sub-sections.

Physical deposition techniques

Physical deposition techniques use mechanical, electromechanical or thermodynamic means to deposit a thin film from solid form. High quality films can be deposited using one of the techniques in high vacuum deposition conditions (Beke 2011). Various physical deposition techniques are as follows:

Thermal evaporation technique

Most of the authors have adopted thermal evaporation technique for ZnTe thin film deposition (Ibrahim et al. 2004; Ibrahim 2006; Hsu et al. 2013; Hussain et al. 2018; Yoshino et al. 2002; Kalita et al. 1999). In this technique, resistive heating melts the material to be deposited and raise vapors of depositing material towards substrate in a high vacuum chamber ($\approx 10^{-3}$ – 10^{-5} Pa). It is a simple, low-cost, scalable and reproducible technique to deposit thin films of excellent purity over large substrate area. Physical properties like deposition rate, temperature and thickness can be controlled (Ibrahim et al. 2004). Thin film depositions at vacuum ranging from typical 3×10^{-2} – 10^{-5} Pa have been reported. Deposition rates of 0.5 to 3–5 nm/s have been reported (Ibrahim 2006; Bacaksiz et al. 2009; Rao et al. 2009; Jeetendra et al. 2014; Raju et al. 1992). It has been observed that ZnTe thin films of various thickness viz. 85 nm (Hsu et al. 2013), 300 nm (Ibrahim 2006; Yoshino et al. 2002; Jeetendra et al. 2014), 300–600 nm (Ibrahim et al. 2004), 300–900 nm (Rao et al. 2009) and ≈ 2000 nm (Raju et al. 1992) can be deposited using thermal evaporation technique. It can be observed from Table 1 that this technique can be applied at below and above room temperature under different vacuum conditions. Thickness of the film can also be controlled by controlling the rate of deposition.

e-beam evaporation technique

In this technique, target is bombarded with an electron beam under high vacuum conditions. The impact of the e-beam helps in transforming atoms from the target into the gaseous phase. Then these atoms precipitate into a thin film form. Similar to thermal evaporation technique, this technique is also requiring high vacuum conditions. It is reported that ZnTe thin films are deposited at vacuum pressure of $\sim 10^{-5}$ Pa– 10^{-4} Pa. Deposition rate can also be controlled, reported values are 0.1, 2.05 and 8 nm/s (Salem et al. 2008; Hossain et al. 2008; Mahmood et al. 2015). It has been observed that ZnTe thin films of various thicknesses can be prepared using this technique viz.

150 nm (Hossain et al. 2008) and 564–880 nm (Salem et al. 2008).

Closed space sublimation (CSS) technique

In CSS technique, depositing material is evaporated and vapor species move and condense onto a substrate surface closely located above source. This technique is a fast, low cost and utilizes the depositing material more efficiently, due to small distance between source and the substrate. But, thickness control is poor due to very fast rate of atoms impinging on substrate. Various researchers (Mahmood and Shah 2014; Aqili et al. 2012; Potlog et al. 2012; Farooq et al. 2014) utilized CSS technique for deposition of ZnTe thin films. It has been observed that ZnTe thin films with 500 nm thickness are deposited by CSS technique (Aqili et al. 2012; Potlog et al. 2012).

Pulsed laser deposition (PLD) technique

PLD is a physical vapor deposition (PVD) technique which is based on ablation process. A pulsed laser beam is focused with an energy density (E_d) on target of depositing material. The reported values for E_d are 0.78 J/cm² (Lastra et al. 2014), 0.82 J/cm² (Erlacher et al. 2005) and 0.8 J/cm² (Lee et al. 2015). The material get vaporized and converted into plasma. This plasma plume deposits on substrate as a thin film. The whole process is performed in high vacuum conditions or in the presence of background gas. It is a simple and versatile technique therefore; many researchers have applied this technique for film formation. Various types of lasers such as excimer laser (Lastra et al. 2014) and Nd: YAG (Erlacher et al. 2005; Lee et al. 2015) has been employed by researchers at different wavelengths ranging from 248 to 1064 nm. ZnTe thin films of various thicknesses are reported, using PLD technique viz. 83 ± 7 nm (Lastra et al. 2014), 250 nm (Lee et al. 2015) and 2300 ± 300–2800 ± 400 nm (Erlacher et al. 2005).

Molecular beam epitaxy (MBE)

In this technique, monolayer is deposited on substrate at a time. In compound deposition, firstly one of the elements is deposited (by repeatedly applying a layer) and then a layer of the other element is deposited. The beam of material can be originated by either chemical reaction (chemical beam epitaxy) or any physical means. It is a slow and laborious technique and the equipment used is complex and very expensive. Binary and quasi-quaternary thin films are reported by MBE technique (Franta et al. 2004; Nakasu et al. 2015; Ueta and Hommel 2002; Chang et al. 2002). Franta et al. (2004) deposited binary thin films on (100) GaAs single crystal substrates, with substrate temperature

maintained at 300 °C. The thickness of these thin films is reported in the range 10–799 nm. Nakasu et al. (2015) also deposited binary ZnTe thin films (thickness = 3.5 nm) on *a*-plane sapphire substrates. Elemental Zn and Te are source materials with 99.9999% purity. The substrate temperature was maintained at 340 °C. The film thickness and growth rate were kept constant at 1 μm and 0.5 μm/h respectively. Ueta and Hommel (2002) have grown ZnMgSeTe quasi-quaternary and ZnCdSeTe layers on (001) ZnTe substrates. The growth temperature was set at 330 °C. Chang et al. (2002) have grown Zn_{0.8}Mg_{0.2}Se_{0.12}Te_{0.88} layers on p-type ZnTe (001) substrates with 260–330 °C substrate temperature range.

Sputtering technique

In sputtering technique, particles are ejected from a solid target material with bombardment by energetic particles such as gas ions. Sputtered species have typical energies depending on the nature of the target, their atomic mass, and the type and energy of the bombarding ions/particles (Beke 2011). It is an economical, widely used and low temperature deposition technique and would be potentially suitable for large area flat panel displays (Zhang et al. 2013). It is observed that amorphous thin films with thickness varying from 128 to 477 nm corresponding to growth time variation from 5 min to 30 min are reported (Zhang et al. 2013). Also, crystalline thin films, having thickness in the range 255–1650 nm (depending upon the r.f. power varying from 50 to 300 W) are deposited using sputtering technique (Bellakhder et al. 2001).

Chemical deposition techniques

In chemical deposition technique, thin film is grown when fluid precursor go through a chemical change at substrate surface. As the precursor encompasses the solid surface, the deposition happens on each part, with minimal regard to direction. The films on large area can deposited with economical cost. Various chemical deposition techniques are as follows:

Brush plating technique

Brush plating technique uses a hand held portable tool for deposition of thin films. It is also known as contact plating, selective plating or swab plating. Plating is applied by means of a swab or brush, soaked with solution and connected to a flexible anode cable (Mohan and Venkataliam 1998). This technique has been applied using aqueous solution of 0.5 M ZnSO₄ and 50 mM TeO₂ as precursor solutions to prepare ZnTe film of thickness 1.5–2.5 μm (Murali et al. 2006).

Table 1 Different parameters of ZnTe thin films deposited by various methods

S. no.	Deposition pressure (Pa)	Substrate temperature (°C)	Optical bandgap (eV)	Structural and morphological parameters Crystallite/grain size, D (nm)	Electrical parameters		Remarks ϵ = relative permittivity μ = mobility ($\text{cm}^2 \text{V}^{-1} \text{s}^{-1}$) R_d/R_i = ratio resistance in dark to resistance in illumination	References	
					Resistivity, ρ ($\Omega \text{ cm}$)	Activation Energy, E_a (eV)			
Thermal evaporation technique									
1	3×10^{-2}	– 123	2.13	46	32	–	Cubic	Bacaksiz et al. (2009)	
		27	2.16	52	1.0×10^4	–			
2	10^{-5}	27	–	37.9	1538	–	$\mu = 12.8$	Rao et al. (2009)	
		100	–	43.3	709	–	$\mu = 21.2^2$		
		200	–	50.3	310	–	$\mu = 36.9^2$		
		280	–	55.2	287	–	$\mu = 37.6^2$		
3	6.6×10^{-3}	30	2.10	10.5	–	0.05	Cubic, average lattice constant = 0.6114 nm, refractive index = 2.50–2.65	Raju et al. (1992)	
		100	2.15	30.5	–	0.07			
		200	2.20	36.0	–	0.09			
		250	2.26	41.0	–	0.04			
		300	2.28	46.0	–	0.11			
4	10^{-3}	Room temperature	–	50–80	2.5×10^4 – 1.7×10^7	–	Cubic, ohmic and SLSC conduction	Ibrahim et al. (2004)	
5	1.3×10^{-3}	27	–	37.9	1538	–	$\mu = 12.8$, $R_d/R_i = 3.73$	Rao et al. (2010a)	
		100	–	43.3	709	–	$\mu = 21.2$, $R_d/R_i = 5.23$		
		200	–	50.3	310	–	$\mu = 36.9$, $R_d/R_i = 15.33$		
		280	2.26	55.2	287	–	$\mu = 37.6$, $R_d/R_i = 21.11$		
S. no.	Deposition pressure (Pa)	Deposition rate (nm/s)	Optical parameters Band gap, E_g (eV) and refractive index, n		Structural and morphological parameters Particle size, D (nm)	Remarks	References		
e- beam evaporation technique									
1	8×10^{-5}	8	$E_g = 2.265$ $n = 2.548$		26.1	Cubic Strain, $\xi = 8.6 \times 10^{-3} \text{Lin}^{-2} \text{m}^{-4}$	Salem et al. (2008)		
2	8×10^{-4}	2.05	–		–	Amorphous, p type with Activation energy = 0.484–1.035 eV	Hossain et al. (2008)		
3	1.3×10^{-4}	0.1	2.24		–	Cubic, Raman peaks at 203–607 cm^{-1}	Mahmood et al. (2015)		
S. no.	Deposition pressure (Pa)	Substrate temperature (°C)	Source temperature (°C)	Optical parameters Band gap, E_g (eV) Refractive index, n		Structural and morphological parameters Grain size, D (nm)	Electrical parameters Resistivity, ρ ($\Omega \text{ cm}$)	Remarks	References
Closed space sublimation technique									
1	10^{-2}	350	450	2.23	–	420	1.01×10^6	Cubic, Raman peak at 314 cm^{-1} , no void or pinholes	Mahmood and Shah (2014)
2	1	400	600	2.24	2.71	300	4.5×10^6	Cubic, Surface roughness = 16–18 nm, Activation Energy = 0.63 eV	Aqili et al. (2012)
3	–	420	590	2.259–2.256	–	–	–	Cubic, no cracks or pinholes	Potlog et al. (2012)
4	1	450	500	2.23	2.27	–	2.91×10^8	Cubic, less porosity, p type, positive hall coefficient	Farooq et al. (2014)

Table 1 continued

S. no.	Deposition pressure (Pa)	Wavelength (nm)	Optical band gap, E_g (eV)		Remarks	References			
Pulsed laser deposition technique									
1	1.3×10^{-7}	248	-		Cubic, Sheet resistance = $2.52 \times 10^{10} \Omega/\text{sq}$ Resistivity = $2.26 \times 10^5 \Omega \text{ cm}$	Lastra et al. (2014)			
2	$< 10^{-4}$	532 1064	1.25 1.32		Amorphous Cubic, crystalline	Erlacher et al. (2005)			
3	1.3×10^{-4}	266	-		Cubic, Raman peaks at $210\text{--}614 \text{ cm}^{-1}$, Semi insulating resistivity	Lee et al. (2015)			
S. no.	Deposition pressure (Pa)	Sputtering gas	Optical parameters		Structural and morphological study	Electrical parameters	Remarks	References	
			Band gap, E_g (eV)	Refractive index, n	Crystallite/grain size, D (nm)	Resistivity, ρ (Ωcm)	Activation Energy, (eV)		
Sputtering technique									
1	1.5–1.6	N_2	1.70	-	19	1.4×10^4	-	Cubic, crystalline Rakhshani (2013)	
2	10^{-2}	Ar	2.26	2.55	213	-	0.48	Cubic, crystalline, resistance = $0.0872\text{--}8.0 \times 10^{11} \Omega$ Bellakher et al. (2001)	
S. no.	Technique name	pH	Optical bandgap (eV)		Structural and morphological parameters		Electrical parameters	Remarks	References
					Grain/crystallite size, D (nm)	Zn:Te		T_c = texture coefficient	
Chemical deposition techniques									
1	Brush plating technique	2.0	2.30	40.0–100.0	49.5:51.5	Resistivity, $\rho = 10^3\text{--}10^4 \Omega\text{cm}$, Carrier concentration, $p = 10^{14}\text{--}10^{15} \text{ cm}^{-3}$, Mobility, $\mu = 5\text{--}60 \text{ cm}^2 \text{ V}^{-1} \text{ s}^{-1}$	Cubic, crystalline, p type	Murali et al. (2006)	
2	SILAR technique	10.0	2.75–3.15	-	53:47	-	Nanocrystalline, no pinholes or cracks	Kale et al. (2007)	
3	Electro-chemical technique	2.5	2.26	35.5–44.9	50.18:49.82	-	Cubic, crystalline, $T_c = 2.12\text{--}2.83$	Mahalingam et al. (2012)	

Electrodeposition technique

Electrochemical deposition is one of the suitable techniques to deposit continuous and semiconducting thin films. This technique has many advantages such as low temperature processing, control of film thickness and morphology, economical etc. (Mahalingam et al. 2002a). It has been observed that ZnTe thin films with thickness (0.1–0.7 μm) are reported (Mahalingam et al. 2002a). This technique requires less starting capital investment and provides great production rates with few limitations of shape and size. Mahalingam et al. (Mahalingam et al. 2012) used electrodeposition technique for thin film deposition.

Other techniques

Some other techniques such as, Successive ionic layer adsorption and reaction method (SILAR) (Kale et al. 2007), Chemical Vapor Deposition (CVD) (Baghchesara et al. 2015), Metal–Organic Chemical Vapor Deposition (MOCVD) (Shan et al. 2002), Metalorganic vapour phase epitaxy (MOVPE) (Nishio et al. 1999) and Spray Pyrolysis (De Merchant and Cocivera 1996) were also reported for depositing ZnTe thin films.

Characterization techniques of ZnTe

The bulk and thin films are characterized for crystallinity, size, structure and other properties so as to investigate its utilization in various applications. In this section, various

optical and electrical characterization techniques, used to study ZnTe thin films have been discussed.

Optical characterization

The optical study of thin film provides information regarding optical transmission, absorption and reflection properties and correlation, if any among these properties to the optical constants of thin film. Various researchers used UV–Vis spectroscopy and PL spectroscopy to study optical properties of ZnTe.

UV–Vis spectroscopy

Absorbance of chalcogenide materials strongly lies in visible region of electromagnetic spectrum with absorption coefficient of the order of 10^4 cm^{-1} . Generally, absorption coefficient of semiconductors in pure state drops rapidly in near or infra-red region and material becomes quite transparent at longer wavelength. Absorption of light can instigate various kind of transitions. These transitions are responsible for the shape of absorption peaks in spectra. To determine the optical band gap (E_g), the absorption coefficient (α) is calculated from transmission curves using relation (Sharma et al. 2017b):

$$\alpha = \frac{1}{d} \ln \left(\frac{1}{T} \right) \quad (1)$$

where, d and T are thickness of film and transmittance respectively. The band gap and absorption coefficient relation is given by (Rao et al. 2009):

$$(\alpha h\nu)^{\frac{1}{r}} = A(h\nu - E_g) \quad (2)$$

where, E_g is band gap, r is the index with values 2, 3, 1/2 and 3/2 for allowed indirect transitions, forbidden indirect transitions, allowed direct transitions and forbidden direct transitions respectively. A is a constant that depends on the transition probability. Now, for direct band gap materials Eq. (2) can be written as,

$$(\alpha h\nu)^2 = A(h\nu - E_g) \quad (3)$$

A typical transmission spectrum for chalcogenide thin films is shown in Fig. 1. Envelop method is generally applied to find refractive index (n) using interference minima and maxima observed at a wavelength from the transmission spectra and band gap can be estimated from $(\alpha h\nu)^2$ versus $h\nu$ plots by extrapolating straight line portion of curves to $h\nu$ axis (Mahalingam et al. 2012; Singh et al. 2018d).

$$n = [N + (N^2 - n_s^2)]^{\frac{1}{2}} \quad (4)$$

$$N = \frac{n_s^2 + 1}{2} + \frac{2n_s(T_{\max} - T_{\min})}{T_{\max}T_{\min}} \quad (5)$$

where n_s is refractive index of substrate, T_{\min} and T_{\max} are the minimum and maximum transmittances of the fringes.

Photoluminescence (PL) spectroscopy

This spectroscopy is a non-destructive and contactless technique to explore the electronic structure of samples. PL is used to estimate material quality by finding the defect levels, deep and shallow impurities in the samples. The electrons residing in valence band are excited by external energy source. These electrons emit light energy with de-excitation of electrons i.e. electrons coming back from conduction band to valence band (ground state).

PL Spectroscopy is of two types i.e. intrinsic PL and extrinsic PL, depending on the nature of electronic transition producing it. Intrinsic luminescence owes to recombination of an electron and a hole, with absence of any external incorporated impurities or defects. It has three sub types: (i) band to band luminescence, (ii) exciton luminescence and (iii) cross luminescence. Extrinsic luminescence is caused by intentionally incorporated impurities, mostly metallic impurities or defects. In most of practical applications, extrinsic luminescence is observed. It has two types: (i) unlocalized and (ii) localized. In pure samples, the photon energy with formation of excitons at low temperature is given as (Jayakrishnan 2008).

$$h\nu = E_g - E_x \quad (6)$$

where E_x denotes excitonic binding energy.

Electrical characterization

The electrical characterization of ZnTe thin films includes measurement of conductivity/resistivity of material. These measurements are done in dark (dark conductivity) and in presence of light (photoconductivity) as a function of temperature and intensity of light. In transient photoconductivity, rise and decay of photocurrent is studied on illumination with light as a function of time as shown in Fig. 2.

Effects of deposition methods on optical, structural and electrical properties of ZnTe thin films

Researchers used various physical and chemical deposition techniques such as thermal evaporation, e-beam evaporation, closed space sublimation, pulsed laser deposition, molecular beam epitaxy and electrodeposition technique, etc. to deposit ZnTe thin films as explained thoroughly in “ZnTe Deposition Techniques” section. Presently the effects of deposition methods on optical, structural,

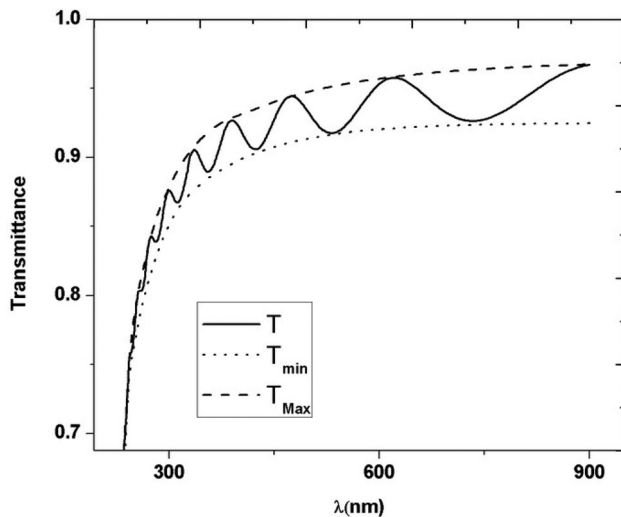


Fig. 1 Typical transmission spectra of chalcogenide thin film

morphological and electrical properties of ZnTe thin films have been presented in detail.

Thermal evaporation technique

Various parameters of ZnTe thin films, deposited by various researchers using thermal evaporation technique are represented in Table 1. It is well understood that various properties of ZnTe thin films can be controlled by adjusting the deposition pressure and substrate temperature. Different studies revealed that thermal evaporated thin films under mostly similar vacuum conditions were polycrystalline in nature with cubic zinc blende structure (Ibrahim et al. 2004; Ibrahim 2006; Hsu et al. 2013; Hussain et al. 2018; Yoshino et al. 2002; Kalita et al. 1999; Bacaksiz et al. 2009; Rao et al. 2009; Jeetendra et al. 2014; Raju et al. 1992; Rao et al. 2010a). Direct band gap (E_g) values were found to be substrate temperature and film thickness dependent. It was observed that E_g value increases with increase in substrate temperature (Bacaksiz et al. 2009; Raju et al. 1992) but Rao et al. (2009) reported that E_g decreased with increasing substrate temperature due to improvement in crystallinity and stoichiometry at higher temperatures (Table 1). Jeetendra et al. (2014) reported decrease in band gap value with increase in film thickness. Crystallinity of thin films improved with raising substrate temperature suggested by increase in grain size (Rao et al. 2009; Raju et al. 1992; Rao et al. 2010a). Electrical study showed that ZnTe films are p-type (Rao et al. 2009). Ohmic, SLSC, Schottky and Poole-Frenkel conduction mechanisms were reported (Ibrahim et al. 2004; Ibrahim 2006; Rao et al. 2009). Mobility, carrier concentration and conductivity improved with increasing substrate temperature attributed to improvement in grain size at elevated temperatures (Table 1) (Rao et al. 2009, 2010). The ratio of

film resistance under dark (R_d) and illuminated conditions (R_i) increased as photoresponse improved with increasing substrate temperature (Rao et al. 2010a).

e-beam evaporation technique

Salem et al. (2008), Hossain et al. (2008) and Mahmood et al. (2015) deposited polycrystalline ZnTe thin films using e-beam evaporation technique. ZnTe thin films were polycrystalline with cubic structure (Salem et al. 2008; Mahmood et al. 2015) whereas, Hossain et al. (2008) obtained amorphous ZnTe films with 150 nm thickness (Table 1). In this method deposition pressure and deposition rate are two main controlling parameters. Particle size, lattice constant, refractive index and activation energy increased as thickness of film increased whereas band gap and strain have opposite effect (Raju et al. 1992; Hossain et al. 2008).

Closed space sublimation technique

Various researchers deposited ZnTe thin films under low to moderate vacuum conditions (Mahmood and Shah 2014; Aqili et al. 2012; Farooq et al. 2014). The developed thin films were polycrystalline in nature with cubic structure without any cracks or pin holes (Mahmood and Shah 2014; Aqili et al. 2012; Potlog et al. 2012; Farooq et al. 2014). Band gap and refractive index values are given in Table 1. P-type (Farooq et al. 2014) films show electrical resistivity of the order of $10^6 \Omega\text{cm}$ for substrate-source temperature difference of 100–200 °C (Mahmood and Shah 2014; Aqili et al. 2012), but high resistivity of order of $10^8 \Omega\text{cm}$ was observed for films developed with substrate-source temperature difference of 50 °C (Farooq et al. 2014). Study revealed that substrate-source temperature difference play important role in controlling the properties of thin films.

Pulsed laser deposition technique

Under high vacuum conditions, PLD technique was applied to develop crystalline, cubic thin film (Lastra et al. 2014; Lee et al. 2015; Achharya et al. 2007). Lastra et al. (Lastra et al. 2014) used excimer laser (KrF, $\lambda = 248 \text{ nm}$) with energy density ($E_d = 0.78 \text{ J/cm}^2$) in $1.3 \times 10^{-7} \text{ Pa}$ vacuum to grow crystalline ZnTe thin films. The source and substrate were separated by 6.5 cm distance with deposition rate of 0.1 nm/s. Erlacher et al. (Erlacher et al. 2005) deposited thin films at two different wavelengths i.e. $\lambda_{\text{pld}} = 532 \text{ nm}$ and $\lambda_{\text{pld}} = 1064 \text{ nm}$ using Nd: YAG laser. It was found that films had amorphous dominating portion which may be due to absence of substrate heat treatment. Films grown at $\lambda_{\text{pld}} = 1064 \text{ nm}$ showed some crystallinity with zincblende structure. Lee et al. (Lee et al. 2015)

deposited ZnTe films on sapphire substrate using Nd: YAG laser at $\lambda_{\text{pld}} = 262$ nm. The repetition frequency of the laser was 10 Hz. Films were crystalline cubic in nature. Target and substrate heater were separated by 7 cm. Substrate was kept at 250 °C.

Molecular beam epitaxy technique

MBE technique was used to deposit crystalline ZnTe thin films at different substrate temperatures (Table 1). Franta et al. (2004) deposited ZnTe thin film on GaAs single crystal substrate. The flux of Zn and Te atoms was monitored by a reference gauge. The beam equivalent pressure was $1.3\text{--}2.6 \times 10^{-5}$ and $5.3\text{--}21.3 \times 10^{-5}$ Pa for Zn and Te respectively. Nakasu et al. (2015) used Zn (6 N pure) and Te (6 N pure) to deposit on sapphire substrate with thickness of 3.5 nm at 100 °C. The growth rate and film thickness was maintained at 0.5 $\mu\text{m}/\text{h}$ and 1 μm respectively. Quasi-quaternary films were also reported using MBE technique (Ueta and Hommel 2002; Chang et al. 2002). 30 nm thick crystalline films were reported deposited at substrate temperature in 300–370 °C range with Raman peaks observed at 204.5, 411.1 and 614.6 cm^{-1} (Zhang et al. 2015). The photoluminescence spectra with emission peaks at 2.121–2.377 eV and crack density in the range $4.8 \times 10^7\text{--}1.3 \times 10^8 \text{ cm}^{-3}$, were measured based on intensity of Zn and Te beams (Nakasu et al. 2017).

Sputtering technique

Sputtering technique was used under low/moderate vacuum conditions to coat ZnTe thin films (Späth et al. 2005; Gessert et al. 1995). Nitrogen and Argon were used as sputtering gases (Bellakhder et al. 2001; Rakhshani 2013). Films were crystalline in nature having cubic lattice structure. Optical band gap and refractive index had values 2.26 and 2.55 eV, respectively for films deposited at r.f. power equals to 250 W (Bellakhder et al. 2001). Electrical resistivity, carrier concentration, mobility and activation energy were also calculated (Table 1) (Bellakhder et al. 2001; Rakhshani 2013). Zhang et al. (Zhang et al. 2013) deposited amorphous ZnTe thin films with nanocrystalline embedded using magnetron sputtering. Pulse frequency was fixed at 40 kHz. The sputtering pressure and current was maintained at 5 Pa and 1 A, respectively.

Chemical deposition technique

Various chemical deposition techniques such as Brush plating (Murali et al. 2006), SILAR (Kale et al. 2007) and electro-chemical (Mahalingam et al. 2012) were reported for depositing ZnTe thin films with different pH values. The films had cubic structure. Murali et al. (2006) reported

deposition of p-type films with composition of Zn:Te = 49.5:51.5. 270 nm thick film with composition Zn:Te = 53:47 had shown $E_g = 3.15$ eV (Kale et al. 2007). All the observations are given in Table 1.

Different physical and chemical deposition techniques are discussed. It was observed that maximum optical band gap value ($E_g = 2.28$ eV) among various physical deposition techniques was obtained from Thermal evaporation technique depending upon its deposition conditions (Raju et al. 1992). Similarly brush plated technique provides utmost optical band gap, $E_g = 2.30$ eV among chemical deposition techniques (Murali et al. 2006). All techniques provide polycrystalline thin films with cubic structure. Only thin films prepared by thermal evaporation technique are incorporated to study ohmic, SLSC, Schottky and Poole-Frenkle conduction mechanisms (Ibrahim et al. 2004; Ibrahim 2006; Rao et al. 2009).

Effect of annealing on optical, structural and electrical properties of ZnTe thin films

Annealing is a heat treatment that amends optical, structural and electrical properties of materials. Annealing improves the crystallinity of material as grain growth occurs during annealing process. The optical and electrical properties can easily elevate with improvement in optical band gap and conductivity, respectively. Hence, annealing plays important role in achieving high performance devices. Also, annealing environment plays an important role in controlling various properties of thin films. ZnTe thin films were annealed at various temperatures under different annealing atmospheres. The effect of annealing on optical, structural, morphological and electrical properties of ZnTe thin films is described in Table 2. ZnTe thin films were annealed in air (Mahalingam et al. 2002b; Bhatti et al. 2004; Raj and Xavier 2013), vacuum (Farooq et al. 2014; Garcia et al. 2000), Argon (Kashyout et al. 1997; Bacaksiz et al. 2009; Shanmugan et al. 2009), Nitrogen (Aqili et al. 2011; Hossain et al. 2015) and Zn (Yoshino et al. 2004) environments for different time periods. Most of the films remain crystalline with cubic structure when annealed at different temperatures (Table 2) (Bacaksiz et al. 2009; Farooq et al. 2014; Mahalingam et al. 2002b; Raj and Xavier 2013; Aqili et al. 2011) whereas Hsu et al. (2013) obtained hexagonal structure and Shanmugan et al. (2009) reported presence of mix phase of hexagonal and orthorhombic along with cubic phase. Bacaksiz et al. (2009) reported that optical band gap increased with annealing which was attributed to grain growth and crystallinity improvement. Also the film texture was randomized with annealing. Electrical resistivity was reduced with increase in annealing temperature with improvement in carrier concentration. Aqili et al. (2011) annealed the ZnTe

thin films at 400 °C for 1 h under nitrogen pressure range 10^4 – 10^5 Pa. Optical band gap and refractive index reduced which might be due to doping during annealing in Nitrogen environment. Te atoms might be replaced by nitrogen atoms which resulted in decrease in Te ratio (Table 2). It was observed that films lose transparency and smoothness with increase in nitrogen pressure during annealing. Resistivity decreased with annealing whereas dark activation energy also reduced with heat treatment which indicated a rise in nitrogen concentration and strong interaction among impurities. Farooq et al. (2014) also found small decrease in optical band gap and electrical resistivity with annealing in vacuum at 380 °C for 1 h. P-type, polycrystalline films (as deposited and annealed) showed improved refractive index after annealing. Hossain et al. (2015) annealed ZnTe thin films for 1 h in temperature range of 300–425 °C under nitrogen ambient. P-type (as deposited and annealed) ZnTe films had lower band gap value as annealing temperature was increased, which is attributed to improvement in crystallinity after annealing (Table 2). SEM images showed smooth and crack free surface with large granular shaped identical grains after annealing at 425 °C. This showed the improvement in crystallinity of ZnTe thin films with grain growth due to annealing of thin films. Kashyout et al. (1997) annealed ZnTe thin films in argon atmosphere for 10 min by varying temperature from 350 to 400 °C. It was observed that transmittance and optical band gap increased as annealing temperature rose from 350 to 400 °C. At 350 °C, low transmittance and band gap (1.80 eV) was observed which attributed to presence of significant amount of Te elemental in thin film. The thin films grown from elemental Te to Cubic ZnTe as annealing temperature is raised from 350 to 400 °C. With increase in grain size upon annealing, Hall mobility for majority carriers also increased. Mahalingam et al. (2002) annealed ZnTe thin films in air for 1 h at 350 °C. It was observed that optical band gap of ZnTe thin films increased from 1.90 to 2.25 eV upon annealing at 350 °C which was attributed to removal of excess unbound Te content in films. Sharp and intense peaks suggested improved crystallinity after annealing. Coarse grained structure turned into smooth surface with reduced intergranular spacing on air annealing. Shanmugan et al. (2009) studied annealing effect on structural properties of ZnTe thin films prepared by Stacked Elemental Layer (SEL) method. ZnTe thin films were annealed at different temperatures from 200 to 425 °C for 1 h under argon gas atmosphere. XRD results revealed that films were polycrystalline with mixed phases of Orthorhombic and Hexagonal ZnTe, along with peaks of elemental (Zn and Te) at low annealing temperature (200 °C). At maximum annealing temperature (425 °C), hexagonal phase changes to cubic ZnTe but hexagonal phases of ZnTe and Te still existed suggesting that Zn

atoms were present at stack surface when annealed at high temperature. Hsu et al. (2013) reported that ZnTe thin films were crystalline having hexagonal structure on annealing at 600, 700 and 800 °C in an rapid thermal annealing (RTA) system for 1 min. Less intense diffraction peaks were observed at 800 °C due to higher surface kinetic energies produced by maximum annealing temperature damaging the microstructure. The grain size and uniformity improved on annealing and was temperature dependent. Raj and Xavier (2013) annealed ZnTe thin films in air for 15 min at temperature range 50–200 °C. It was observed that absorption, crystallinity and photoconductivity of ZnTe thin films improved with annealing up to 150 °C and attributed to smoothness of film attained after annealing. Activation energy decreased with increasing annealing temperature. Film decomposed and lost its crystallinity with annealing at 200 °C. Bhatti et al. (2004) air annealed ZnTe thin films for 15 min at various temperatures (100–375 °C). Optical properties of annealed ZnTe thin films had been studied. The band gap value slightly increased with rise in annealing temperature.

Garcia et al. (2000) studied annealing effect on photoluminescence of ZnTe thin films excited at 514 nm with 10 K cooling conditions. ZnTe thin films were annealed in vacuum (9.3×10^{-3} Pa) for 4 h at different annealing temperatures (200, 300 and 400 °C). As deposited sample had PL emission in excitonic range at 520, 522, 526 and 532–536 nm correspond to recombination of free excitons, Cu impurities, Zn vacancies and free to bound and donor–acceptor emissions, respectively. Similarly, deep level emission spectra band at 551–564 nm was attributed to donor–acceptor band where Cu was an acceptor. Emissions at 575 and 598 nm were related to structural and grain boundary defects, respectively. Red emission observed at 660 nm was related to oxygen centres. With annealing, the free exciton line decreased in excitonic range corresponding to nonradiative centres created by annealing, which can capture excitons and change the crystalline quality of sample. The intensity of peak at 522 nm (Cu impurities) improved as annealing temperature increased. This was attributed to formation of shallow acceptor centers by dissociation and diffusion of Cu complex or other aggregates. For emission spectra in deep level region, the intensity of peak at 575 nm increased for 200 °C, reduced at 300 °C and peak disappeared at 400 °C. With increasing annealing temperature, increase in intensity of DA_{Cu} band (donor–acceptor band) and appearance of new emission at 586–588 nm was observed (Raj and Xavier 2013). An emission band at 650 nm was also seen for annealing at 400 °C. Yoshino et al. (Yoshino et al. 2004) studied the annealing effect in Zn atmosphere (0.77–34 Pa). ZnTe thin films were annealed at 600 °C for 400 h. PL observed at 4.2 K for as deposited films had four peaks at 2.382 eV due to free exciton related to lower polaritons,

Table 2 Effect of annealing on optical, structural, morphological and electrical properties of ZnTe thin films

S. no.	Annealing atmosphere T = time	Annealing temperature (°C)	Annealing effect on		Structural and morphological parameters Crystallite/grain size, D (nm)	Electrical parameters Resistivity, ρ (Ωcm)	Remarks S.R. = sheet resistance ($\Omega/\text{sq.}$) N_t = trap density (cm^{-3}) ε = strain ($\text{Lin}^{-2} \text{m}^{-4}$) T_c = texture coefficient E_a = activation energy (eV)	References
			Optical parameters Band gap, E_g (eV)	Band gap, E_g (eV)				
1	RTA, T = 1 min	As deposited	–	–	–	–	–	Hsu et al. (2013)
		600	–	–	–	–	Hexagonal along (003) (103) (112) (113)	
		700	–	–	–	–	Hexagonal, S.R. = 9300	
		800	–	–	–	–	Hexagonal, oriented along (101) (102) (112)	
2	Argon, T = 30 min	As deposited	2.16	–	52.00	1.0×10^4	Crystalline, most intense at (111)	Bacaksiz et al. (2009)
		200	–	–	–	–	Intense at (111),	
		300	–	–	–	–	Less intense at (111),	
		400	2.23	–	65.00	6.2×10^3	Least intense at (111) along with (200) (240) (311)	
3	Nitrogen T = 1 h	As deposited	2.248 ± 0.001	–	–	$2.50 \times 10^7 \pm 5 \times 10^5$	Cubic, $E_a = 0.74$	Aqili et al. (2011)
		400	2.247 ± 0.001	–	–	$9.4 \times 10^4 \pm 1900$	$E_a = 0.41$	
		As deposited	–	–	–	2.91×10^8	Cubic, Polycrystalline, p-type, positive hall coefficient	Farooq et al. (2014)
		380	–	–	–	2.29×10^7	–	Hossain et al. (2015)
5	Nitrogen, T = 1 h	As deposited	2.25	–	–	–	Te elemental film, small grains	
		300	2.21	–	–	–	Te elemental film, moderate grain size	
		350	2.15	–	–	–	Te elemental film, enlarge grains	
		425	2.00	–	–	–	Cubic, ZnTe film, enlarged grains	
6	Argon, T = 10 min	As deposited	–	–	–	–	–	Kashyout et al. (1997)
		350	1.80 ± 0.1	–	–	–	Zn/Te = 0.6 , S.R. = $29.5 \times 10^3 \pm 2$	
		375	2.26 ± 0.1	–	–	–	Zn/Te = 0.9 , S.R. = $110.13 \times 10^3 \pm 5$	
		400	2.31 ± 0.1	–	–	–	Zn/Te = 1.0 , S.R. = $815 \times 10^3 \pm 5$	
7	Air, T = 1 h	As deposited	1.90	–	–	–	Sharp peaks, coarse grain, P type, $N_t = 3.6 \times 10^{15}$	Mahalingam et al. (2002)
		350	2.25	–	–	–	More sharp and intense peaks	
		As deposited	–	–	–	–	–	Shanmugan et al. (2009)
		425	–	–	–	–	–	
8	Argon, T = 1 h	As deposited	–	–	–	–	–	
		200	–	–	–	–	Hexagonal and orthorhombic	
		275	–	–	–	–	Hexagonal	
		350	–	–	10.26	–	Hexagonal, $\varepsilon = 20.21 \times 10^{-2}$, $T_c = 1.55$	
425	–	–	17.88	–	Cubic and Orthorhombic, $\varepsilon = 11.60 \times 10^{-2}$, $T_c = 1.47$			

Table 2 (continued)

S. no.	Annealing atmosphere T = time	Annealing temperature (°C)	Annealing effect on		Structural and morphological parameters Crystallite/grain size, D (nm)	Electrical parameters Resistivity, ρ (Ωcm)	Remarks S.R. = sheet resistance (Ω/sq.) N _t = trap density (cm ⁻³) ε = strain (Lin ⁻² m ⁻⁴) T _c = texture coefficient E _a = activation energy (eV)	References
			Optical parameters Band gap, E _g (eV)	Deep level emission wavelength (nm)				
9	Air, T = 1 h	As deposited	2.23	-	-	-	-	Raj and Xavier (2013)
		50	-	-	-	E _a = 2.64		
		100	-	-	-	E _a = 2.37		
		150	-	-	-	E _a = 1.92		
		200	-	-	-	E _a = 2.21		
10	Air, T = 15 min	As deposited	2.15	-	-	-	-	Bhatti et al. (2004)
		100	2.18	-	-	-		
		200	2.20	-	-	-		
		250	2.22	-	-	-		
		300	2.25	-	-	-		
11	Vacuum 9.3 × 10 ⁻³ Pa, T = 4 h	As deposited	2.26	-	-	-	-	Garcia et al. (2000)
		200	Near band gap emission wavelength (nm)	Deep level emission wavelength (nm)	-	PL, excitation wavelength = 514.0 nm		
		300	520–536	551–660	-	-		
		400	522	575	-	-		
		-	-	550–588	-	-		
12	Zn, 0.7–34 Pa, T = 400 h	As deposited	522	-	-	-	-	Yoshino et al. (2004)
		600	PL emission (eV)	Refractive index, n	-	PL excitation = 325.0–441.6 nm		
		-	2.34–2.38	-	-	-		
-	-	-	2.31–2.38	-	-	-	-	

2.381 eV for upper polaritons, 2.379 eV because of radiative recombination of excitons bound to neutral donors and 2.375 eV for neutral acceptors in band-edge region. DAP (donor-to-acceptor pair) and FA (free-to-acceptor) emissions observed at 2.334 and 2.343 eV, respectively were related to residual impurities when annealed at 600 °C for 400 h, the peaks at 2.382, 2.381 and 2.379 eV disappeared as Zn vapor pressure increased. Whereas intensity of peak at 2.375 eV decreased with Zn vapour pressure and also disappeared at high pressure which might be due to substitution of Zn atoms in V_{Zn} site. The intensity of DAP emission decreased below 2.8 Pa and improved with increase in Zn vapor pressure due to change in recombination from between V_{Zn} acceptor and V_{Te} donor, to between Zn_i donor and Te_i acceptor. Te precipitates appeared in as deposited films reduced and disappeared with annealing under Zn pressure beyond 50 Pa.

The study revealed that annealing had an enhancing impact on optical, structural and electrical properties of ZnTe thin films. For optical study, it can be concluded that annealing improved the transmittance of ZnTe thin films. Enhancement in optical band gap value with annealing was reported by many researchers (Kashyout et al. 1997; Bacaksiz et al. 2009; Mahalingam et al. 2002b; Bhatti et al. 2004; Hossain et al. 2015) except few authors (Farooq et al. 2014; Aqili et al. 2011; Hossain et al. 2015) whose results show slight decrease in E_g with annealing due to improvement in crystallinity and annealing in nitrogen ambient. Similarly in structural and morphological study, the improvement in crystallinity, grain size/crystallite size of ZnTe thin films was observed after annealing (Kashyout et al. 1997; Bacaksiz et al. 2009; Mahalingam et al. 2002b; Raj and Xavier 2013; Hossain et al. 2015). It was studied that Te elemental films grown into Cubic ZnTe films after annealing (Hossain et al. 2015). Also phase conversion from hexagonal to cubic phase was observed after annealing (Shanmugan et al. 2009). Annealing effect on electrical study showed that resistivity reduced with increase in carrier concentration and mobility for p-type ZnTe thin films (Kashyout et al. 1997; Bacaksiz et al. 2009; Aqili et al. 2011). Films annealed in nitrogen ambient showed that dark conductivity activation energy decreased with increase in nitrogen pressure (Aqili et al. 2011). Increase in photoconductivity was also observed (Raj and Xavier 2013).

Effect of doping on optical, structural, morphological and electrical properties of ZnTe thin films

Doping is intentional addition of impurity to tailor the various properties of a material. With incorporation of impurity atoms the crystallinity and electrical conductivity

of material get affected up to good extent (Mahmood et al. 2015; Gul et al. 2014; Rao et al. 2010b). Optical properties also vary with doping as dopant atom replace parent atom from its crystal structure. Doping enhances the applicability of chalcogenides. ZnTe thin films have been doped with different elemental compositions. The effect of different dopants on optical, structural, morphological and electrical properties of ZnTe thin films is studied and the observations are given in Table 3.

Indium doping

Pattar et al. (2009) doped amorphous ZnTe thin films with Indium by immersing in the solution containing 1 g $(In(NO_3)_3 \cdot 5H_2O)$ in 1 litre H_2O . The ZnTe thin films were immersed for different times (5, 10 and 15 min). It was observed that optical band gap lowered as doping concentration was increased which might be due to incorporation of Indium into ZnTe thin films. With heat treatment, the amorphous film was grown into crystalline film with increasing doping level. Grain growth and improved crystallite size with less strain was observed. Doping also enhanced the electrical conductivity of ZnTe thin films due to increase in mobility and carrier concentration. Pal (1993) doped ZnTe thin films with indium (6 wt%) using vacuum evaporation technique. Improvement in electrical conductivity was observed after doping.

Copper doping

Lastra et al. (2014) doped ZnTe thin film by immersing in 6, 7, 9, 11, 13, 15 and 60 mg $Cu(NO_3)_2 \cdot 3H_2O$ in 150 ml deionized H_2O for 1 min. After doping films were heated at 200 and 300 °C for 10 min. Structural study revealed that the undoped films have only cubic phase with preferential orientation along the (1 1 1) plane. It has been observed that the thin films (immersed in 15 mg $Cu(NO_3)_2 \cdot 3H_2O$ and annealed at 200 °C), exhibits hexagonal phase at $2\theta = 44.55^\circ$ in XRD pattern. For the same sample, the hexagonal phase disappeared with annealing at 300 °C but orthorhombic phase was observed at $2\theta = 27.45^\circ$. The cubic phase is also observed in annealed sample (at 200 and 300 °C) with preferential orientation along the (1 1 1) plane. This might be due to copper atoms incorporation in grain boundaries of ZnTe/ZnTe:Cu. Mobility and carrier concentration improved with increasing doping level whereas sheet resistance and resistivity of doped thin films reduced at 300 °C annealing temperature (Table 3). Gul et al. (2014) doped ZnTe thin films with copper (0, 6, 8 and 10 at.%) using thermal evaporation technique. Optical band gap decreased (from 2.24 to 1.64 eV) with increasing doping content (0–10 at.%) which was attributed due to Cu incorporation forming solid solution. Cu-doped films had

shown higher refractive index which was due to decrease in crystallite boundaries, improved crystallinity and packing density (Table 3). With substitution of Zn atom with Cu, blue shift from 194 to 203 cm^{-1} in fundamental LO (longitudinal optical phonon mode) was observed in Raman spectra. No significant change in crystal structure was observed on doping. Improvement in crystallinity was seen from sharp and intense diffraction peaks after doping. Mahmood et al. (2014) doped ZnTe thin films by immersing in solution containing 1 g copper in 1 l of distilled water. Films were immersed for different times (5, 10, 15 and 20 min). Optical study showed decrease in transmission from 80% (undoped) to 67% (20 min immersion). Decrease in optical band gap was observed which attributed to defects after doping as the localized states density was reduced in band structure. Structural study of doped films revealed that crystallite size was improved due to Cu diffusion. No peak corresponding to Cu was observed in diffraction pattern. Intensity of dominant peak was reduced due to disturbance in crystal structure. As-deposited and annealed films had smooth, dense void free surface. Compositional analysis showed that Cu replaced Te with little rise in Zn concentration. It was reported that electrical resistivity reduced with doping with improvement in crystal structure due to less micro structural defects (Table 3). Reduced mobility after doping was also reported.

Nitrogen doping

Lee et al. (2015) doped ZnTe using pulsed laser deposition under different partial pressure of N_2 gas (13×10^{-3} Pa, 6.6 and 9.3 Pa). It was found that the intensity of Raman modes of doped samples decreased with annealing due to decrease in crystallinity of ZnTe thin films. Lattice constant varied from 6.08 to 6.13 Å as N ions were placed in interstitial sites. Electrical results showed that mobility and resistivity decreased whereas hole concentration increased with increasing doping level (from 6.6 to 9.3 Pa N_2 pressure) due to high concentration of $(\text{N})_{\text{Te}}$ defects in ZnTe thin films.

Nickel doping

Mahmood et al. (2015) deposited $\text{Zn}_{1-x}\text{Ni}_x\text{Te}$ thin films using electron beam evaporation technique with different compositions ($x = 0.05, 0.10, 0.15$ and 0.20). Linear fall in optical band gap with increasing doping concentration was reported due to incorporation of Ni into ZnTe thin films. Diffraction angle of polycrystalline cubic thin films shifted to smaller angle values with increasing doping content and the lattice constant also increased (Table 3). This also confirmed the formation of ternary compound. Increase in

grain size and decrease in micro strain was also observed with increasing Ni concentration. EDAX spectra showed that peak corresponding to Ni increased with increase in doping content. Decrease in Zn peak was attributed to substitution of Zn atoms by Ni atoms in the crystal lattice.

Chromium doping

Sharma et al. (2013) deposited chromium doped $\text{Zn}_{1-x}\text{Cr}_x\text{Te}$ alloy thin films with thermal evaporation technique using $x = 0.1$ and 0.2 . Slight decrease in absorbance was observed with incorporation of Cr atoms. A linear decrease in band gap was observed with increase in Cr doping (Table 3). Doped films had mix phase of Cubic and Hexagonal ZnTe structure. I–V characteristics showed improvement in electrical conductivity.

Bismuth doping

Rao et al. (2010) doped vacuum deposited ZnTe thin films with new technique of using nano-spheres, where dopant material is used in form of nano-spheres. ZnTe thin film was vacuum deposited on pre-deposited discontinuous bismuth film having bismuth nano-spheres. This technique was found to be effective as proper diffusion of dopant was achieved. Different concentrations of bismuth were used (0.18, 0.23 and 0.32 at.%). No significant change in optical band gap was reported after doping. The electrical parameters changed with increasing dopant concentration. Increase in carrier concentration was attributed to increase in bismuth atoms. Marginally decrease in hole mobility was reported due to increase in ionized impurities as it disrupt the charge carriers flow. Decrease in resistivity and activation energy with increasing doping content was also observed (Table 3, Rao et al. 2010b).

Silver doping

Aqili et al. (2012) doped ZnTe thin films by immersing in solution containing 1 g AgNO_3 in 1 l H_2O for 1, 5 and 30 min respectively. Films were annealed at 400 °C for 1 h. With high Ag doping concentration, band gap decreased and refractive index increased. In diffraction pattern, no peak for Ag was observed but peaks of Ag_2Te monoclinic structure appeared with high doping concentration. AFM results revealed almost same grain size for all samples due to same deposition parameters for all thin film samples (Table 3). Dark activation energy reduced on increasing annealing temperature due to strong interaction among impurities. The electrical resistivity decreased attributed to silver atoms diffusion in the entire film. Mahmood et al. (2014) doped ZnTe thin films by immersing in solution containing 1 g Ag in 1 l of distilled

Table 3 Effect of doping on optical, structural, morphological and electrical properties of ZnTe thin films

S. no.	Dopant	Doping	Heat treatment	Doping effect on				References
				Optical band gap, E_g (eV)	Structural and morphological parameters Crystallite/grain size, D (nm)	Electrical parameters Resistivity, ρ (Ωcm)	Remarks n = refractive index LO = longitudinal optical phonon mode ϵ = micro strain δ = dislocation density S.R. = sheet resistance E_a = activation energy	
1	Indium	Undoped	127 °C, 3 h	2.37	–	–	Amorphous	Pattar et al. (2009)
		5 min immersion	127 °C, 3 h 10^{-1} Pa	–	13.0	–	Crystalline, $\epsilon = 3.04 \times 10^{-3} \text{ lin}^{-2} \text{ m}^{-4}$ $\delta = 5.86 \times 10^{15} \text{ lin m}^{-2}$	
		10 min immersion	127 °C, 3 h 10^{-1} Pa	–	14.8	–	Crystalline, $\epsilon = 2.44 \times 10^{-3} \text{ lin}^{-2} \text{ m}^{-4}$ $\delta = 4.545 \times 10^{15} \text{ lin m}^{-2}$	
		15 min immersion	127 °C, 3 h 10^{-1} Pa	2.14	–	–	–	
2	Indium	Undoped	–	–	–	7.10×10^6	Polycrystalline, p type	Pal (1993)
		6 wt. %	127 °C, 6 h	–	–	3.00×10^5		
3	Copper 'x' mg of $\text{Cu}(\text{NO})_3 \cdot 3\text{H}_2\text{O}$ in 150 ml deionized H_2O	Undoped	–	–	–	2.26×10^5	Cubic, orientation along (111) (220), S.R. = $2.52 \times 10^{10} \Omega/\text{sq}$. S.R. = $1.60 \times 10^7 \Omega/\text{sq}$. S.R. = $5.80 \times 10^6 \Omega/\text{sq}$. S.R. = $1.38 \times 10^6 \Omega/\text{sq}$. S.R. = $2.70 \times 10^5 \Omega/\text{sq}$. S.R. = $4.88 \times 10^5 \Omega/\text{sq}$. Cubic, (111) (220) Orthorhombic Cu_xTe at (052) S.R. = $3.90 \times 10^4 \Omega/\text{sq}$. S.R. = $3.90 \times 10^4 \Omega/\text{sq}$.	Lastra et al. (2014)
		x = 6 mg	300 °C, 10 min	–	–	145.00		
		x = 7 mg	300 °C, 10 min	–	–	50.00		
		x = 9 mg	300 °C, 10 min	–	–	12.45		
		x = 11 mg	300 °C, 10 min	–	–	2.44		
		x = 13 mg	300 °C, 10 min	–	–	4.39		
		x = 15 mg	300 °C, 10 min	–	–	0.35		
		x = 60 mg	300 °C, 10 min	–	–	0.35		
4	Copper	Undoped	–	2.24	64.7	–	Cubic, n = 2.39, LO = 194 cm^{-1} n = 2.47, LO = 199 cm^{-1} n = 3.03, LO = 201 cm^{-1} n = 3.20, LO = 203 cm^{-1}	Gul et al. (2014)
		6 at. %	–	2.00	66.3	–		
		8 at. %	–	1.84	67.4	–		
		10 at. %	–	1.64	67.7	–		
5	Copper	Undoped	–	2.23	420.0	1.01×10^6	Cubic, visible transmission = 80% Visible transmission = 67%	Mahmood and Shah (2014)
		20 min immersion	350 °C, 1 h, 10^{-2} Pa vacuum	2.21	490.0	68.97		

Table 3 (continued)

S. no.	Dopant	Doping	Heat treatment	Doping effect on			References	
				Optical band gap, E_g (eV)	Structural and morphological parameters Crystallite/grain size, D (nm)	Electrical parameters Resistivity, ρ (Ωcm)		Remarks n = refractive index LO = longitudinal optical phonon mode ε = micro strain δ = dislocation density S.R. = sheet resistance E_a = activation energy
6	Nitrogen	Undoped	–	–	–	–	Most intense Raman modes, polycrystalline	Lee et al. (2015)
		13.3 mPa	–	–	–	–	Intensity of Raman modes dec., crystallinity dec.	
		6.6 Pa	–	–	–	54.90	Intensity of Raman modes dec., crystallinity dec.	
		9.3 Pa	–	–	–	9.32	Intensity of Raman modes dec., crystallinity dec.	
7	Nickel	Undoped	–	2.25	–	–	Cubic, Zn:Te:Ni = 45.26:54.70:0.00	Mahmood et al. (2015)
		5%	–	–	–	–	Zn:Te:Ni = 43.61:51.53:4.83	
		10%	–	–	–	–	Zn:Te:Ni = 40.66:50.26:9.06	
		15%	–	–	–	–	Zn:Te:Ni = 35.33:51.71:12.97	
		20%	–	–	–	–	Zn:Te:Ni = 31.23:50.02:18.73	
8	Chromium	Undoped	–	2.57	–	–	Cubic and hexagonal	Sharma et al. (2013)
		0.1	–	1.84	–	–	Hexagonal	
		0.2	–	1.47	–	–	Hexagonal	
9	Bismuth	Undoped	–	2.25	–	1.32×10^3	$E_a = 0.89$ eV	Rao et al. (2010b)
		0.18 at. %	–	2.25	–	1.19×10^2	–	
		0.23 at. %	–	2.25	–	0.88×10^2	–	
		0.32 at. %	–	2.25	–	0.85×10^2	$E_a = 0.78$ eV	
10	Silver	Undoped	–	2.24	–	4.50×10^6	Cubic, crystalline,	Aqili et al. (2012)
		(1 min immersion)	1 Pa, 400 °C, 1 h	2.21	–	8.10×10^3	p type, n = 2.71, $E_a = 0.63$ eV $E_a = 0.42$ eV	
		(5 min immersion)	1 Pa, 400 °C, 1 h	2.18	–	5.90×10^2	$E_a = 0.25$ eV	
11	Silver	(30 min immersion)	1 Pa, 400 °C, 1 h	2.16	–	3.54	$E_a = 0.14$ eV	Mahmood and Shah (2014)
		Undoped	–	2.23	420.0	1.01×10^6	Cubic, visible transmission = 80%, no pinholes	
		20 min immersion	350 °C, 1 h, 10^{-2} Pa vacuum	2.19	430.0	4.00×10^4	Visible transmission = 60%, no pinholes	

Table 3 (continued)

S. no.	Dopant	Doping	Heat treatment	Doping effect on				References
				Optical band gap, E_g (eV)	Structural and morphological parameters Crystallite/grain size, D (nm)	Electrical parameters Resistivity, ρ (Ωcm)	Remarks n = refractive index LO = longitudinal optical phonon mode ε = micro strain δ = dislocation density S.R. = sheet resistance E_a = activation energy	
12	Gadolinium	Undoped	–	~ 2.26	30.0	–	Oriented along (111) (200) (311) (400) (422) (511)	Ma et al. (2008)
		3 at.%	N ₂ , 400 °C, 30 min	–	–	–	Oriented along (111) (200) (311) (400) (422) (511)	
		7 at.%	N ₂ , 400 °C, 30 min	–	–	–	Oriented along (111)	
		8 at.%	N ₂ , 400 °C, 30 min	~ 2.28	–	–	Oriented along (111) (311)	
		9 at.%	N ₂ , 400 °C, 30 min	~ 2.31	15.0	–	Cubic, oriented along (111) (311)	
13	Vanadium	Undoped (150 nm thickness)	–	–	–	–	Temperature range = 300–332 K, E_a = 0.50 eV	Hossain et al. (2008)
		2.5 wt.%	–	–	–	–	E_a = 0.48 eV	
		5.0 wt.%	–	–	–	–	E_a = 0.46 eV	
		7.5 wt.%	–	–	–	–	E_a = 0.42 eV	
		10.0 wt.%	–	–	–	–	E_a = 0.36 eV	

water for different time periods (5, 10, 15 and 20 min). It was found that transmission of doped ZnTe thin films in visible spectra decreased with doping. Decrease in band gap was observed due to presence of more defect states. Crystallite size also reduced with doping because the diffusion energy of Ag layer on thin films was not attained, which resulted in decrease in diffusion length of atoms and increase in defects. Slight increase in grain size indicated coalescence phenomenon. Decrease in electrical resistivity was observed due to improvement in crystal structure and decrease in structural defects. Decrease in mobility after doping was also observed (Table 3).

Gadolinium doping

Ma et al. (2008) doped up to 10% Gd into ZnTe thin films using laser-assisted deposition/epitaxy technique. Results showed that optical band gap improved with increasing doping content except for 7 at.% Gd doping. Structural results showed that grain size reduced from ~ 30 nm (as deposited) to ~ 15 nm (7 at.% doped sample). Most of the diffraction

peaks disappeared except (111) up to 7 at.% Gd doped samples as the defect sites were reduced due to Gd bonding and other domains were suppressed. However, with increase in doping concentration, (311) domain became dominant due to additional defects like defect complexes.

Vanadium doping

Amorphous Vanadium doped thin films were deposited by Hossain et al. (2008). Films were doped by e-beam evaporation technique with different concentration of V varying from 0 to 10 wt%. It was observed that activation energy decreased with increase in doping concentration for films of thickness 150 nm (Table 3). This indicated that conduction was taking place in the states near the Fermi level for highly doped samples whereas carriers were activated to participate in conduction mechanism for less doped ZnTe thin films.

Doping effect on optical, structural, morphological and electrical properties of ZnTe thin films was studied. Optical results showed that transmittance and optical band gap decreased due to incorporation of dopant atoms in crystal

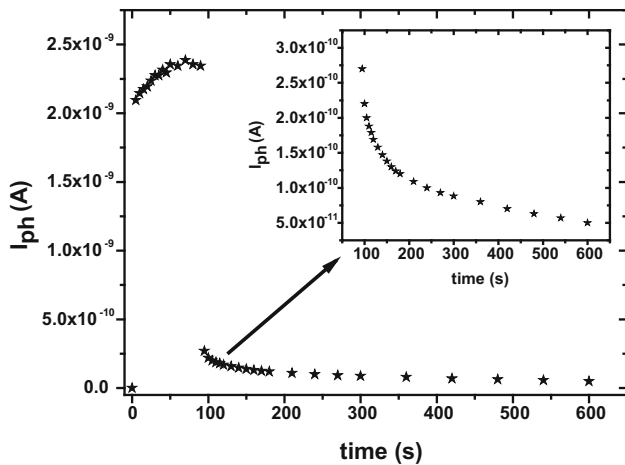


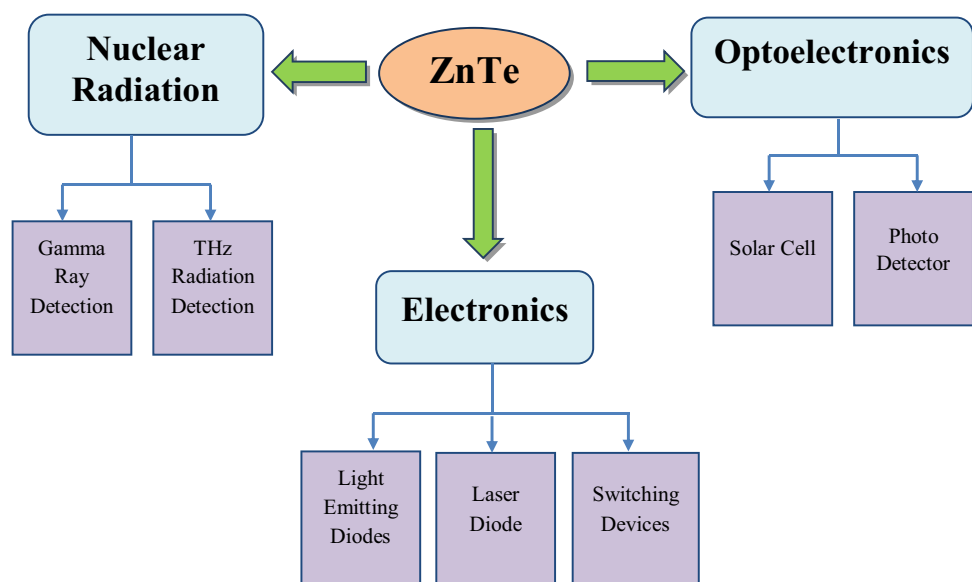
Fig. 2 Rise and decay current for a chalcogenide thin film

structure (Mahmood et al. 2015; Mahmood and Shah 2014; Aqili et al. 2012; Gul et al. 2014; Sharma et al. 2013) however some researchers found no effect (Rao et al. 2010) or improvement in optical band gap after doping (Pattar et al. 2009; Ma et al. 2008). Structural and morphological study showed improvement in crystallinity leading to lower strain after doping (Mahmood et al. 2015; Mahmood and Shah 2014; Pattar et al. 2009). Few authors reported decrease in crystallinity (Lee et al. 2015) and amorphous films (Hossain et al. 2008). Electrical results showed increase in conductivity and carrier concentration whereas resistivity, sheet resistance, mobility and activation energy lowers with doping (Hossain et al. 2008; Aqili et al. 2012; Lastra et al. 2014; Pal 1993; Rao et al. 2010). However non-linear behaviour of carrier concentration and mobility was observed with increasing doping concentration (Lastra et al. 2014).

Applications and future scope of ZnTe thin films

ZnTe applications in different fields are given in Fig. 3. Zinc telluride is commonly used semiconducting materials in optoelectronics devices (Ibrahim 2006; Kalita et al. 1999; Salem et al. 2008; Erlacher et al. 2005; Achharya et al. 2007; Sarma et al. 2006). Due to low cost and high absorption coefficient, ZnTe is used in photovoltaic and photoelectrochemical cells (Hossain et al. 2008). ZnTe thin films and Zn-rich alloy films like ZnCdTe are used in making of pure-green (Hussain et al. 2018; Yoshino et al. 2002; Ueta and Hommel 2002; Chang et al. 2002; Rao et al. 2010) and green-yellow light emitting diodes, photodetectors (Yoshino et al. 2002), laser diodes (Ueta and Hommel 2002) and used in tandem solar cell applications (Gashin et al. 1997; Rohatgi et al. 1989) and quantum well structures (Kalita et al. 1999). ZnTe thin film is successfully used in Gamma ray detectors (Wang et al. 1994), terahertz radiation detectors (Wennewisser et al. 1997; Liu et al. 2002), switching devices (Ota and Takahashi 1973), transparent heating elements and electromagnetic field coatings (Bhatti et al. 2004). It is also used as back contact for CdTe in CdTe/CdS heterojunction solar cells to obtain high efficiency (Späth et al. 2005; Gessert et al. 1995; Feng et al. 1996). It can be used to synthesize ternary semiconductor compounds like $Cd_xZn_{(1-x)}Te$ and optical band gap can be attuned by varying composition x . At visible wavelength, sensor can be protected by Vanadium-doped ZnTe which acts as a non-linear optical photorefractive material. As compare to conventional limiters, Vanadium doped ZnTe limiters are light and compact. High-intensity jamming beam can be blocked by ZnTe:V from

Fig. 3 Applications of ZnTe in different fields



a laser dazzler and can pass a lower-intensity image of the observed scene. For 600–1300 nm wavelength range, better photorefractive performance is observed as comparison to III–V and II–VI group semiconductors. Photorefractive yield can be improved by using manganese as an additional dopant (ZnTe:V:Mn) (Malik 2013). It is also used as electro-optic detector under terahertz radiation which causes it to show optical birefringence and change the polarization of a transmitting light (Malik 2013; Patra and Pardhan 2012).

It has been observed that various research groups have reported the study on optical, structural and electrical properties of ZnTe thin films. But, the compositional dependent study on structural, optical and electrical properties of ZnTe has been limitedly reported. There is a scope to investigate compositional dependent structural, optical and electrical properties of nanocrystalline ZnTe thin films. This kind of study is fruitful in providing the knowledge of structural, optical and electrical properties of ZnTe at different Zn/Te compositions which is essential in fabrication of opto-electronic devices. It has been observed that annealing study is mostly reported for Zn₅₀Te₅₀ thin films. There is a scope to study the annealing effect for other compositions as well. Similarly, composition dependent doping study on various properties of ZnTe has a wide future scope. There is a scope to investigate ZnTe as gamma rays shielding and sensing material as Te exhibit high atomic number ($Z = 52$). The high atomic number and higher density materials are required for shielding and sensing gamma rays due to their higher probability of interaction with materials. Additionally, ZnTe has low melting point, which make easy manufacturing of a shielding material.

Conclusion

ZnTe thin films have been deposited on substrate with different methods. Each method has its own merits and demerits. Quality of films, cost effective, time consumption, easy to operate, thermal conditions and application are the important parameters considered before selection of any deposition technique. Physical deposition techniques provide high quality thin films whereas chemical deposition techniques are used to produce thin films in large extent. Annealing has enhancing effect on optical, structural, morphological and electrical properties of ZnTe thin films depends upon annealing temperature, annealing atmosphere and time period of annealing. Dopants can be added either through physical or chemical (immersion) methods. Similar to annealing, doping also improves the structural, morphological and electrical properties of ZnTe thin films. However optical study shows that band gap is

reduced with doping due to incorporation of dopant atoms in crystallite sites.

Acknowledgements One of the authors (Tejbir Singh) is thankful to SERB (Project No. SR/FTP/PS-081/2012) for the financial assistance.

References

- Abrikosov NK, Bankina VF, Poretskaya LV, Shelimova LE, Skudnova EV (1969) Semiconducting II–VI, IV–VI, and V–VI compounds. Plenum Press, New York
- Achharya KP, Erlacher A, Ullrich B (2007) Optoelectronic properties of ZnTe/Si heterostructures formed by nanosecond laser deposition at different Nd:YAG laser lines. *Thin Solid Films* 515:4066–4069
- Akkad FE, Abdulaheem Y (2013) Morphology, electrical, and optical properties of heavily doped ZnTe: Cu thin films. *J Appl Phys* 114:183501
- Aqili AKS, Ali Z, Maqsood A (2011) Characterization of zinc telluride thin films deposited by two-source technique and post-annealed in nitrogen ambient. *J Cryst Growth* 317:47–51
- Aqili AKS, Saleh AJ, Ali Z, Al-Omari S (2012) Ag doped ZnTe films prepared by closed space sublimation and an ion exchange process. *J Alloys Compd* 520:83–88
- Bacaksiz E, Aksu S, Ozer N, Tomakin M, Özçelik A (2009) The influence of substrate temperature on the morphology, optical and electrical properties of thermal-evaporated ZnTe thin films. *Appl Surf Sci* 256:1566–1572
- Baghchesara MA, Yousefi R, Cheraghizade M, Sheini FJ, Saaedi A (2015) Photocurrent application of Cd-doped ZnTe nanowires grown in a large scale by a CVD Method. *Vacuum* 123:131–135
- Beke S (2011) A review of the growth of V2O5 films from 1885 to 2010. *Thin Solid Films* 519:1761–1771
- Bellakhder H, Outzourhit A, Ameziane EL (2001) Study of ZnTe thin films deposited by r.f. sputtering. *Thin Solid Films* 382:30–33
- Bhargava R (1997) Properties of wide band gap II–VI semiconductors. INSPEC/The Institution of Electrical Engineers, London
- Bhatti MT, Raza MI, Rana AM (2004) Study of the optical properties of ZnTe thin films for use in photovoltaic cells. *J Res (Sci)* 15:369–375
- Chandhuri S, Pal AK (2001) Optical processes in nanocrystalline semiconductor materials. *Proc Natl Sci Acad* 67A:131–143
- Chang JH, Takai T, Godo K, Song JS, Koo BH, Hanada T, Yao T (2002) ZnTe-based light-emitting-diodes grown on ZnTe substrates by molecular beam epitaxy. *Phys Status Solidi B* 229:995–999
- Contreras M, Egaas B, Ramanathan K, Hiltner J, Swartzlander A, Hasoon F, Noufi R (1999) Progress toward 20% efficiency in Cu(In, Ga)Se₂ polycrystalline thin-film solar cells. *Prog Photovolt* 7:311–316
- De Merchant J, Cocivera M (1996) Properties of zinc telluride containing impurities introduced during spray pyrolysis. *J Electrochem Soc* 143:4054–4059
- Erlacher A, Ambrico M, Perna G, Schiavulli L, Ligonzo T, Jaeger H, Ullrich B (2005) Absorption and photoconductivity properties of ZnTe thin films formed by pulsed-laser deposition on glass. *Appl Surf Sci* 248:402–405
- Fang F, Mc Candless BE, Opila RL (2009) Chemical and electrical properties of ZnTe based solar cells. Proceedings of the 34th IEEE Photovoltaic Specialists Conference, pp. 001258-001263, 2009
- Farooq MU, Khan M, Faraz A, Maqsood A, Ahmad W, Li L (2014) Comparative study of ZnTe thin films prepared using close space

- sublimation (CSS) and electron beam evaporation (EBE) thin film fabrication techniques for optoelectronic applications. *Mater Technol* 29:29–35
- Feng L, Mao D, Tang J, Collins RT, Trefny JU (1996) The structural, optical, and electrical properties of vacuum evaporated Cu-doped ZnTe polycrystalline thin films. *J Electron Mater* 25:1422–1427
- Franta D, Ohlídal I, Klapetek P, Ramil AM, Bonanni A, Stifter D, Sitter H (2004) Optical properties of ZnTe films prepared by molecular beam epitaxy. *Thin Solid Films* 468:193–202
- Gangopadhyay U, Kim K, Mangalaraj D, Yi J (2004) Low cost CBD ZnS antireflection coating on large area commercial monocrystalline silicon solar cells. *Appl Surf Sci* 230:364–370
- Garcia JA, Remón A, Muñoz V, Triboulet R (2000) Annealing-induced changes in the electronic and structural properties of ZnTe substrates. *J Mater Res* 15:1612–1616
- Gashin P, Focsha A, Potlog T, Simashkevich AV, Leondar V (1997) n-ZnSe/p-ZnTe/n-CdSe tandem solar cells. *Sol Energy Mater Sol Cells* 46:323–331
- Gessert TA, Mason AR, Reedy RC, Matson R, Coutts TJ, Sheldon P (1995) Development of rf sputtered, Cu-doped ZnTe as a contact interface layer to p-CdTe. *J Electron Mater* 24:1443–1449
- Gessert TA, Sheldon P, Li X, Dunlavy D, Sasala R, Albright S, Zadler B (1997) Studies of ZnTe back contacts to CdS/CdTe Solar cells. *Proceedings of the 26th IEEE Photovoltaic Specialists Conference*, pp. 419–422, 1997
- Gul Q, Zakria M, Khan TM, Mahmood A, Iqbal A (2014) Effects of Cu incorporation on physical properties of ZnTe thin films deposited by thermal evaporation. *Mater Sci Semicond Process* 19:17–23
- Hossain MS, Islam R, Khan KA (2008) Temperature effect on the electrical properties of undoped and vanadium-doped ZnTe thin films. *Renew Energy* 33:642–647
- Hossain MI, Kamruzzaman M, Islam ABMO (2015) Effects of temperature in electrodeposition of ZnTe thin films. *J Mater Sci* 26:1756–1762
- Hsu C-H, Tseng C-F, Yu Y-T, Yang P-C, Lai C-H, Lin J-S, Yang H-W (2013) Effect of annealing temperature on electrical properties of ZnTe layers grown by thermal evaporation. *Adv Mat Res* 608:1314–1317
- Hussain T, Kuhaili MFA, Durrani SMA, Qayyum HA (2018) Influence of angle deposition on the properties of ZnTe thin films prepared by thermal evaporation. *Ceram Int* 44:10130–10140
- Ibrahim AA (2006) DC electrical conduction of zinc telluride thin films. *Vacuum* 81:527–530
- Ibrahim AA, El-Sayed NZ, Kaid MA, Ashour A (2004) Structural and electrical properties of evaporated ZnTe thin films. *Vacuum* 75:189–194
- Ignatowicz S, Kobendza A (1981) *Semiconducting thin films of A^{II}B^{VI} compounds*. Wiley, New York
- Jayakrishnan R (2008) Defect analysis of semiconductor thin films for photovoltaic applications using photo-luminescence and photo-conductivity. Ph.D thesis, Dept. of Physics, Cochin University
- Jeetendra S, Naveen CS, Raghu P, Mahesh HM (2014) Optimization of thickness of ZnTe thin film as back contact for CdTe thin film solar cells. *Int J Eng Res Tech* 3:431–435
- Jiao SJ, Zhang ZZ, Lu YM, Shen DZ, Yao B, Zhang JY, Li BH, Zhao DX, Fan XW, Tang ZK (2006) ZnO p-n junction light-emitting diodes fabricated on sapphire substrates. *Appl Phys Lett* 88:031911
- Kale SS, Mane RS, Pathan HM, Shaikh AV, Joo O-S, Han S-H (2007) Preparation and characterization of ZnTe thin films by SILAR method. *Appl Surf Sci* 253:4335–4337
- Kalita PK, Sarma BK, Das HL (1999) Photoresponse characteristics of vacuum evaporated ZnTe thin films. *Ind J Pure Appl Phys* 37:885–890
- Kashyout AB, Aricò AS, Antonucci PL, Mohamed FA, Antonucci V (1997) Influence of annealing temperature on the opto-electronic characteristics of ZnTe electrodeposited semiconductors. *Mater Chem Phys* 51:130–134
- Kshirsagar SD, Krishna GM, Tewari SP (2013) Optical characteristics of wurtzite ZnTe thin films. *Mater Sci Semicond Process* 16:1002–1007
- Lastra G, Luque PA, Quevedo-Lopez MA, Olivas A (2014) Electrical properties of p-type ZnTe thin films by immersion in Cu solution. *Mater Lett* 126:271–273
- Lee KS, Oh G, Kim EK (2015) Growth of p-type ZnTe thin films by using nitrogen doping during pulsed laser deposition. *J Korean Phys Soc* 67:672–675
- Liu K, Kang H-S, Kim T-K, Zhang X-C (2002) Study of ZnCdTe crystals as terahertz wave emitters and detectors. *Appl Phys Lett* 81:4115–4117
- Liu W, Gu SL, Ye JD, Zhu SM, Liu SM, Zhou X, Zhang R, Shi Y, Zheng YD, Hang Y, Zhang CL (2006) Blue-yellow ZnO homostructural light-emitting diode realized by metalorganic chemical vapor deposition technique. *Appl Phys Lett* 88:092101
- Ma Z, Liu L, Yu KM, Walukiewicz W, Perry DL, Yu PY, Mao SS (2008) Experimental and theoretical studies on gadolinium doping in ZnTe. *J Appl Phys* 103:023711
- Mahalingam T, John VS, Rajendran S, Sebastian PJ (2002a) Electrochemical deposition of ZnTe thin films. *Semicond Sci Technol* 17:465–470
- Mahalingam T, John VS, Rajendran S, Ravi G, Sebastian PJ (2002b) Annealing studies of electrodeposited zinc telluride thin films. *Surf Coat Technol* 155:245–249
- Mahalingam T, Dhanasekaran V, Sundaram K, Kathalingam A, Rhee J-K (2012) Characterization of electroplated ZnTe coatings. *Ionics* 18:299–306
- Mahmood W, Shah NA (2014) Effects of metal doping on the physical properties of ZnTe thin films. *Curr Appl Phys* 14:282–286
- Mahmood A, Shaista R, Shah A, Aziz U, Ahmed E, Ali S, Raza Q (2011) Ellipsometric analysis of Cd_{1-x}Zn_xSe thin films prepared by a thermal evaporation technique. *Phys Scr* 83:065706
- Mahmood A, Rashid R, Aziz U, Shah A, Ali Z, Raza Q, Ashraf T (2015) Structural and optical properties of Zn_{1-x}Ni_xTe thin films prepared by electron beam evaporation technique. *Prog Nat Sci* 25:22–28
- Malik MA (2013) 4.09 – Compound semiconductors: chalcogenides. *Compr Inorg Chem II (Second Edition)* 4:177–210
- Millerd JE, Brock NJ, Brown MS, DeBarber PA, Trivedi S (1996) Resonant holographic interferometry with ZnTe:V:Mn. *Appl Opt* 35:5275–5285
- Mirov SB, Fedorov VV, Moskalev IS, Martyshkin DV (2007) Recent progress in transition-metal-doped II–VI Mid-IR lasers. *IEEE J Sel Top Quantum Electron* 13:810–822
- Mochizuki K, Terano A, Momose M, Taika A, Kawata M, Gotoh J, Nakatsuka S (1995) Crystallographic microstructure and electrical characteristics of Au/Pt/Ti/Ni ohmic contacts on p-type (001) ZnTe layers. *J Appl Phys* 78:3216–3220
- Mohan S, Venkataciialam R (1998) Brush plating - present state of art. *Bull Electrochem* 14:472–475
- Murali KR, Ziaudeen M, Jayaprakash N (2006) Structural and electrical properties of brush plated ZnTe films. *Solid-State Electron* 50:1692–1695
- Nakasu T, Aiba T, Yamashita S, Hattori S, Sun W, Taguri K, Kazami F, Kobayashi M, Asahi T (2015) Control of domain orientation during the MBE growth of ZnTe on a-plane sapphire. *J Cryst Growth* 425:191–194

- Nakasu T, Sun W, Kobayashi M, Asahi T (2017) Effect of Zn and Te beam intensity upon the film quality of ZnTe layers on severely lattice mismatched sapphire substrates by molecular beam epitaxy. *J Cryst Growth* 468:635–637
- Nishio M, Guo Q, Ogawa H (1999) Effect of dopant flow rate upon photoluminescence properties in aluminum-doped ZnTe layers grown by MOVPE. *Thin Solid Films* 343–344:512–515
- Nishio M, Hayashida K, Guo Q, Ogawa H (2001) Effect of VI/II ratio upon photoluminescence properties of aluminum-doped ZnTe layers grown by MOVPE. *Appl Surf Sci* 169:223–226
- Ota T, Takahashi K (1973) Non-polarized memory-switching characteristics of ZnTe thin films. *Solid-State Electron* 16:1089–1096
- Pal U (1993) Dark- and photoconductivity in doped and undoped zinc telluride films. *Semicond Sci Technol* 8:1331–1336
- Patra S, Pardhan SK (2012) Microstructural, optical and quantum confinement effect study of mechanically synthesized ZnTe quantum dots. *Acta Mater* 60:131–138
- Pattar J, Sawant SN, Nagaraja M, Shashank N, Balakrishna KM, Sanjeev G, Mahesh HM (2009) Structural optical and electrical properties of vacuum evaporated indium doped zinc telluride thin films. *Int J Electrochem Sci* 4:369–376
- Potlog T, Maticiu N, Mirzac A, Dumitriu P, Scortescu D (2012) Structural and optical properties of ZnTe thin films. *Proceedings of the International Semiconductor Conference*, pp 321–324, 2012
- Raj CSA, Xavier FP (2013) Effect of post deposition annealing on the optical absorption and photoconductivity studies of pure ZnTe and pure MgPc thin films formed by vacuum deposition. *Arch Appl Sci Res* 5:167–171
- Raju KN, Vijayalakshmi RP, Venugopal R, Reddy DR, Reddy BK (1992) Effect of substrate temperature on the structural, optical and electrical properties of vacuum-evaporated ZnTe films. *Mater Lett* 13:336–341
- Rakhshani AE (2013) Effect of growth temperature, thermal annealing and nitrogen doping on optoelectronic properties of sputter-deposited ZnTe films. *Thin Solid Films* 536:88–93
- Ramanathan K, Contreras MA, Perkins CL, Asher S, Hasoon FS, Keane J, Young D, Romero M, Metzger W, Noufi R, Ward J, Duda A (2003) Properties of 19.2% efficiency ZnO/CdS/CuInGaSe₂ thin-film solar cells. *Prog Photovolt* 11:225–230
- Rao GK, Bangera KV, Shivakumar GK (2009) The effect of substrate temperature on the structural, optical and electrical properties of vacuum deposited ZnTe thin films. *Vacuum* 83:1485–1488
- Rao GK, Bangera KV, Shivakumar GK (2010a) Studies on the photoconductivity of vacuum deposited ZnTe thin films. *Mater Res Bull* 45:1357–1360
- Rao GK, Shivakumar GK, Kasturi VB (2010b) The p-type doping of vacuum deposited ZnTe thin films with bismuth by a new technique of using nano-spheres. *Mater Sci Eng B* 175:185–188
- Rohatgi A, Ringel SA, Sudharsanan R, Meyers PV, Liu CH, Ramanathan V (1989) Investigation of polycrystalline CdZnTe, CdMnTe, and CdTe films for photovoltaic applications. *Sol Cells* 27:219–230
- Ruda HE (1992) *Widegap II-VI compounds for Opto-electronic Applications*. Chapman & Hall, London
- Salem AM, Dahy TM, El-Gendy YA (2008) Thickness dependence of optical parameters for ZnTe thin films deposited by electron beam gun evaporation technique. *Phys B* 403:3027–3033
- Sarma R, Mazumdar N, Das HL (2006) Some spectral response characteristics of ZnTe thin films. *Bull Mater Sci* 29:15–16
- Sato K, Katayama-Yoshida H (2001) Hyperfine interactions and magnetism of 3d transition-metal-impurities in II–VI and III–V compound-based diluted magnetic semiconductors. *Hyperfine Interact* 136:737–742
- Schrier J, Demchenko DO, Wang L, Alivisatos AP (2007) Optical properties of ZnO/ZnS and ZnO/ZnTe heterostructures for photovoltaic applications. *Nano Lett* 7:2377–2382
- Shan CX, Fan XW, Zhang JY, Zhang ZZ, Wang XH, Ma JG, Lu YM, Liu YC, Shen DZ, Kong XG, Zhong GZ (2002) Structural and luminescent properties of ZnTe film grown on silicon by metalorganic chemical vapor deposition. *J Vac Sci Technol* 20:1886–1890
- Shanmugan S, Balaji S, Ramanathan K (2009) Synthesis of ZnTe thin film using stacked elemental layer method: structural studies. *Optoelectron Adv Mater* 3:468–471
- Sharma DC, Srivastava S, Vijay YK, Sharma YK (2013) Preparation and characterization of the chromium doped ZnTe thin films. *Adv Mater Lett* 4:68–70
- Sharma J, Singh H, Singh T (2017a) Study of the mobility activation in ZnSe thin films deposited using inert gas condensation. *J Sci* 2:432–436
- Sharma J, Singh R, Singh H, Singh T, Singh P, Thakur A, Tripathi SK (2017b) Synthesis of SnSe₂ thin films by thermally induced phase transition in SnSe. *J Alloys Compd* 724:62–66
- Sharma J, Singh H, Singh T, Thakur A (2018) Structural, optical and photo-electrical properties of nanocrystalline ZnSe thin films. *J Mater Sci* 29:5688–5695
- Shen Q, Kobayashi J, Diguna LJ, Toyoda T (2008) Effect of ZnS coating on the photovoltaic properties of CdSe quantum dot-sensitized solar cells. *J Appl Phys* 103:084304
- Sidorov YG, Yakushev MV, Pridachin DN, Varavin VS, Burdina LD (2000) The heteroepitaxy of II–VI compounds on the non-isovalent substrates (ZnTe/Si). *Thin Solid Films* 367:203–209
- Singh H, Singh T, Thakur A, Sharma J (2018a) Structural analysis of nanocrystalline ZnTe alloys synthesized by melt quenching technique. *AIP Conf Proc* 1953:030073
- Singh H, Duklan N, Singh T, Thakur A, Sharma J (2018b) Effect of vacuum annealing on structural and optical properties of nanocrystalline ZnTe thin films. *J Mater Sci* 29:4992–4998
- Singh H, Singh P, Thakur A, Singh T, Sharma J (2018c) Nanocrystalline Zn_xTe_{100-x} (x = 0, 5, 20, 30, 40, 50) thin films: structural, optical and electrical properties. *Mater Sci Semicond Process* 75:276–282
- Singh H, Singh T, Thakur A, Sharma J (2018d) Optical parameters of nanocrystalline Zn₄₀Te₆₀ thin films. *Int J Adv Res Sci Eng* 7:214–219
- Smith DJ, Tsen SCY, Chen YP, Faurie JP, Sivanathan S (1995) Microstructure of heteroepitaxial CdTe grown on misoriented Si (001) substrates. *Appl Phys Lett* 67:1591–1593
- Späth B, Fritsche J, Säuberlich F, Klein A, Jaegermann W (2005) Studies of sputtered ZnTe films as interlayer for the CdTe thin film solar cell. *Thin Solid Films* 480–481:204–207
- Tamargo MC (2002) *II-VI semiconductor materials and their applications*. Taylorand Francis, New York
- Tanaka T, Yu KM, Stone PR, Beeman JW, Dubon OD, Reichertz LA, Kao VM, Nishio M, Walukiewicz W (2010) Demonstration of homojunction ZnTe solar cells. *J Appl Phys* 108:024502
- Tanaka T, Ohshita H, Saito K, Guo Q (2018) Photoluminescence of ZnTe/ZnMgTe multiple quantum well structures grown on ZnTe substrates by molecular beam epitaxy. *Superlattices Microstruct* 114:192–199
- Ueta A, Hommel D (2002) New concept for ZnTe-based homoepitaxial light-emitting diodes grown by molecular beam epitaxy. *Phys Status Solidi A* 192:177–182
- Wang YJ, Iwaczyk JS, Patt BE (1994) New concepts for scintillator/HgI₂ gamma ray spectroscopy. *IEEE Trans Nucl Sci* 41:910–914
- Wennewisser C, Jepsen PU, Schall M, Schyja V, Helm H (1997) Electro-optic detection of THz radiation in LiTaO₃, LiNbO₃ and ZnTe. *Appl Phys Lett* 70:3069–3071

- Wu X, Keane JC, Dhere RG, Dehart C, Duda A, Gessert TA, Asher S, Levi DH, Sheldon P (2001) 16.5%-efficient CdS/CdTe polycrystalline thin-film solar cell. Proceedings 17th European Photovoltaic Solar Energy Conference, Munich, pp. 995–1000, 2001
- Yoshino K, Memon A, Yoneta M, Ohmori K, Sato H, Ohishi M (2002) Optical characterization of the ZnTe pure-green LED. *Phys Status Solidi B* 229:977–980
- Yoshino K, Yoneta M, Ohmori K, Saito H, Ohishi M, Yabe T (2004) Annealing effects of a high-quality ZnTe substrate. *J Electron Mater* 33:579–582
- Zhang Z, Li J, Zhang H, Pan X, Xie E (2013) Thickness-dependent field emission from ZnTe films prepared by magnetron sputtering. *J Alloys Compd* 549:88–91
- Zhang L, Liu C, Yang Q, Cui L, Zeng Y (2015) Growth and characterization of highly nitrogen doped ZnTe films on GaAs (001) by molecular beam epitaxy. *Mater Sci Semicond Process* 29:351–356